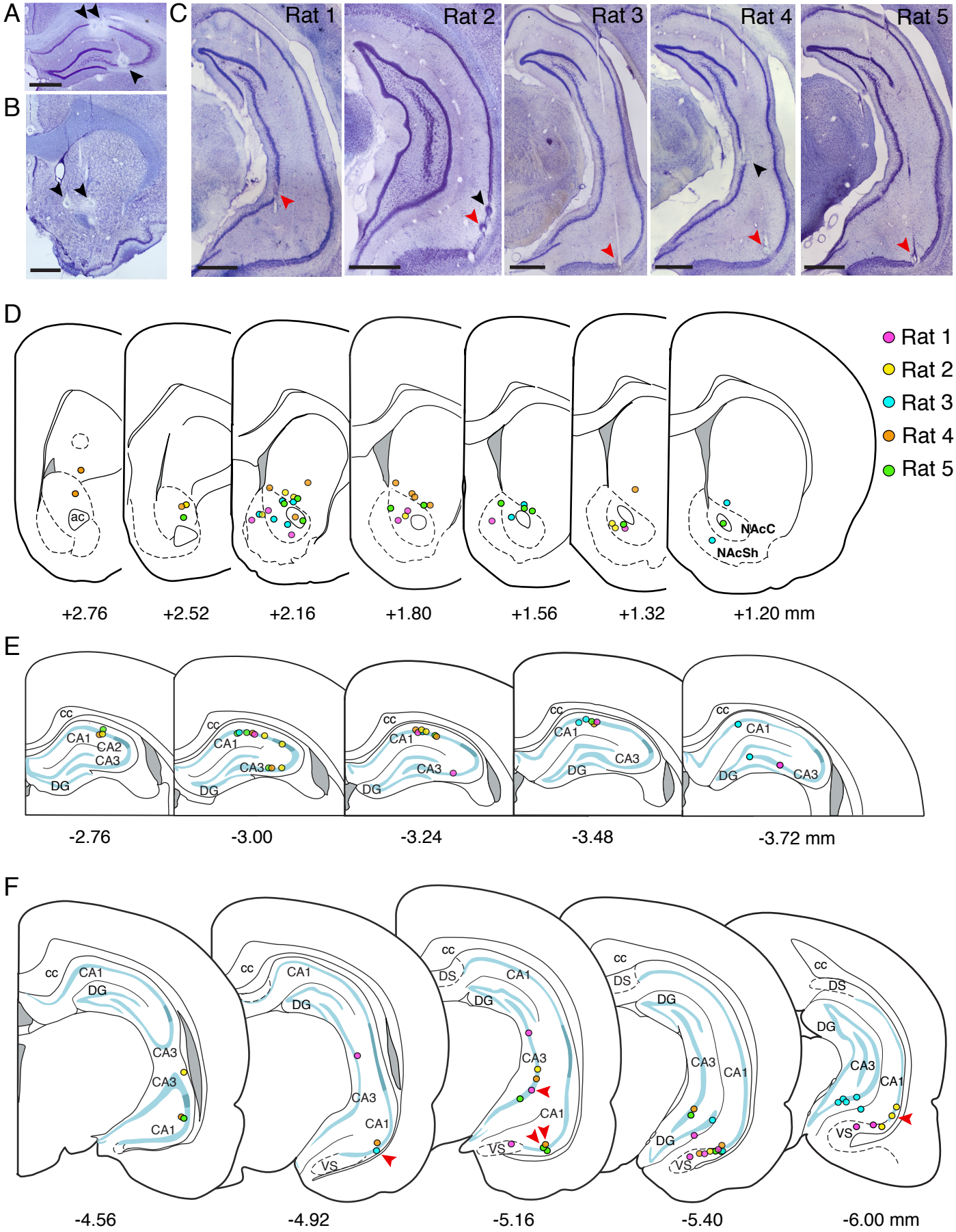
A
B
C
Rat 1
Rat 2
Rat 3
Rat 4
Rat 5
D
ac
NAcC
NAcSh
Rat 1
Rat 2
Rat 3
Rat 4
Rat 5
+2.76
+2.52
+2.16
+1.80
+1.56
+1.32
+1.20 mm
E
cc
CA1
CA2
CA3
DG
-2.76
-3.00
-3.24
-3.48
-3.72 mm
F
cc
CA1
DG
CA3
DS
VS
-4.56
-4.92
-5.16
-5.40
-6.00 mm

Figure S1. Histological identification of recording sites, related to Figure 1A.

(A and B) Nissl-stained coronal sections showing example tetrode lesions marked by black arrows in (**A**) dCA1 and dCA3 and (**B**) NAc, in Rat 5.

(C) Nissl-stained coronal sections showing example tetrode lesions in vH. Each section includes the tetrode used for vSWR detection in each rat (red arrows). In A-C, scale bars are 1 mm.

(D) Summary of all NAc recording locations across rats, aligned to the nearest representative section adapted from the Paxinos & Watson Wistar rat brain atlas (2007). Dots mark the last recorded depth of each tetrode at the end of the experiment. Dotted lines indicate approximate borders of NAc core and shell. Grey shaded regions represent ventricles. All distances are in AP coordinates (mm) relative to Bregma and correspond to original plate labels from the atlas; note that theses distances do not correspond exactly to true recording locations in our Long-Evans rats and are for illustration purposes only. For true implant coordinates, see STAR Methods.

(E and F) Summary of all recording sites in dH (**E**) and vH (**F**). Light blue regions represent stratum pyramidale of CA1/CA3 or granule cell layer of dentate gyrus, darker blue regions represent stratum pyramidale of CA2. Grey shaded regions represent ventricles. Red arrows indicate the 5 sites (1 per animal) used for vSWR detection. Abbreviations: ac, anterior commissure; NAcC, nucleus accumbens core; NAcSh, nucleus accumbens shell; cc, corpus callosum; DG, dentate gyrus; DS, dorsal subiculum; VS, ventral subiculum.

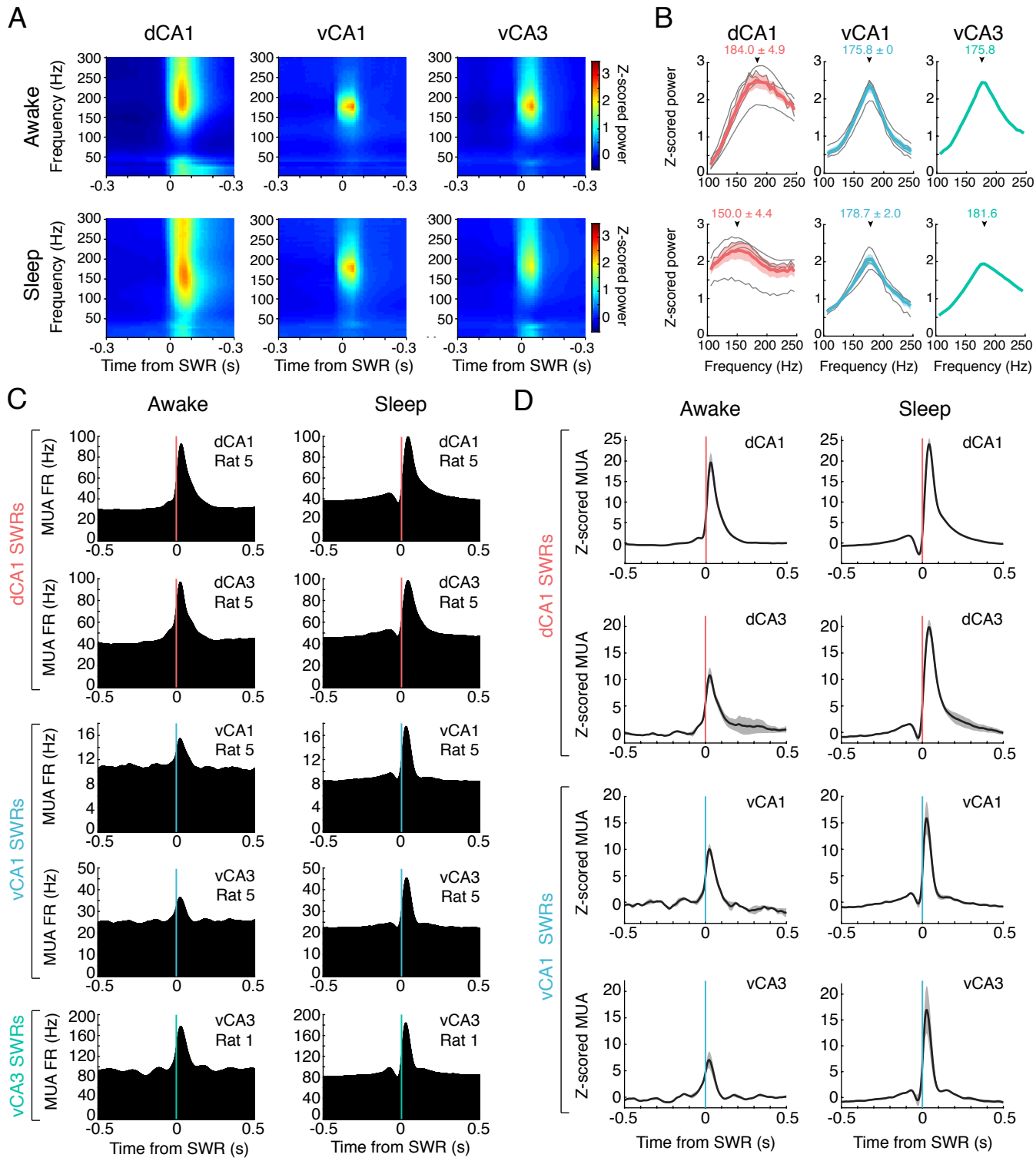
A
dCA1
vCA1
vCA3
Awake
Sleep
Frequency (Hz)
Z-scored power
Time from SWR (s)
B
184.0 ± 4.9
175.8 ± 0
175.8
150.0 ± 4.4
178.7 ± 2.0
181.6
Z-scored power
Frequency (Hz)
C
Awake
Sleep
dCA1 SWRs
vCA1 SWRs
vCA3 SWRs
MUA FR (Hz)
dCA1 Rat 5
dCA3 Rat 5
vCA1 Rat 5
vCA3 Rat 5
vCA3 Rat 1
Time from SWR (s)
D
Awake
Sleep
dCA1 SWRs
vCA1 SWRs
Z-scored MUA
dCA1
dCA3
vCA1
vCA3
Time from SWR (s)
E
Awake
Sleep
Fraction of SWRs
***
SWR amplitude (s.d.)
F
Awake
Sleep
Fraction of SWRs
***
Duration of <4 s.d. SWRs (s)
G
Awake
Sleep
Fraction of epochs
***
SWR rate per epoch (events/s)

Figure S2. Characterization of dH and vH SWRs, related to Figure 1.

(A) Examples of mean SWR-onset-triggered spectrograms on one tetrode from each detection region during awake immobility (top) and sleep (bottom). Left: all dCA1 SWRs in Rat 5 (n=9,642 awake, 26,048 sleep); Center: all vCA1 SWRs in Rat 5 (n=9,672 awake, 31,553 sleep); Right: all vCA3 SWRs in Rat 1, the only rat in which vCA3 SWRs were used (n=18,798 awake, 24,536 sleep). All SWRs >2 s.d. are included. Power is z-scored within each epoch and averaged across epochs and days. In (**A**) and (**B**) SWRs were detected as described in STAR Methods (3 dCA1 tetrodes and 1 vH tetrode per animal).

(B) Mean z-scored power (a slice of the SWR-triggered spectrogram) at frequencies between 100-250 Hz, at the time of peak ripple power for each animal during awake immobility (top row) and sleep (bottom row). Grey curves indicate individual animals, colored curves indicate mean ± s.e.m. across animals. Arrows indicate mean ± s.e.m. peak ripple frequency. Left: dCA1 SWRs (n=51,333 awake, 115,158 sleep, 5 rats); Center: vCA1 SWRs (n=47,222 awake, 120,271 sleep, 4 rats); Right: vCA3 SWRs (n=18,798 awake, 24,536 sleep, 1 rat). As vCA1 and vCA3 SWRs occurred at nearly the same frequency, we pooled these ventral SWRs (vSWRs) for the remainder of the study.

(C) Examples of hippocampal multiunit activity (MUA) in wake and sleep, aligned to the onset of dSWRs (pink lines), vCA1 SWRs (blue lines), or vCA3 SWRs (aqua lines). In the upper right of each panel is the region and rat from which MUA was detected. Firing rate was calculated from the summed spike count from all tetrodes in the region.

(D) Mean z-scored multiunit firing rate at the time of SWRs. Grey shaded region indicates s.e.m across animals. Top two rows: dCA1 and dCA3 MUA aligned to dCA1 SWRs (n=5 rats). Bottom two rows: vCA1 MUA (n=4 rats) and vCA3 MUA (n=3 rats) aligned to vCA1 SWRs. Z-scores were calculated within animal relative to the pre-SWR period (-500 to 0 ms). Strong similarity in activation timing of vCA3 MUA between vCA1 SWRs and vCA3 SWRs (**C**, bottom) also provided support for the use of vCA3 for SWR detection in Rat 1.

(E) Distributions of SWR amplitudes across animals. In both wake and sleep, dSWRs (pink) are typically larger amplitude than vSWRs (blue; ***p=0, Wilcoxon rank-sum test). In **E-G**, only one dCA1 tetrode per animal was used for SWR detection to allow for direct comparison to vSWRs. In (**E**) and (**G**), awake n=54,496 dSWRs, 74,355 vSWRs; sleep n=118,897 dSWRs, 146,995 vSWRs.

(F) Distributions of SWR durations for <4 s.d. SWRs, across animals. In both wake and sleep, dSWRs (pink) are significantly longer than vSWRs (blue), although this difference is more pronounced in sleep (***$p<10^{-40}$, Wilcoxon rank-sum test; awake n=38,170 dSWRs, 71,029 vSWRs; sleep n=66,382 dSWRs, 135,035 vSWRs).

(G) Distributions of dSWR (pink) and vSWR (blue) rate per epoch, expressed as the fraction of epochs with each rate (out of 256 awake epochs and 411 sleep epochs across animals). For awake epochs on the maze, rate was calculated per total time spent at <4 cm/s. For sleep epochs, rate was calculated per time spent in NREM sleep (see STAR Methods). In both wake and sleep, the vSWR rate is typically higher than the dSWR rate (***$p<10^{-40}$, Wilcoxon rank-sum test).

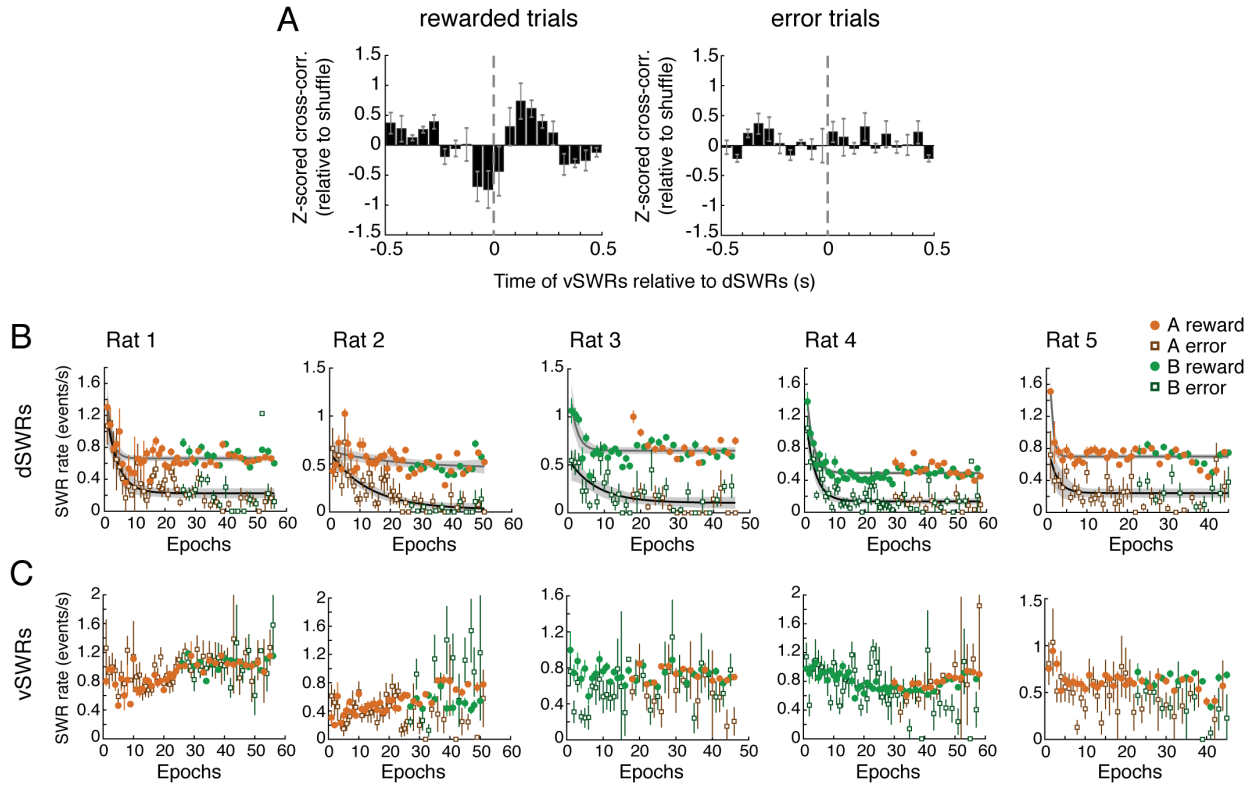

Figure S3. Awake SWR asynchrony and reward modulation, related to Figure 2.

(A) Asynchrony between dSWRs and vSWRs is present on both rewarded (left) and error (right) trials. A minimum of 3 s immobility following the time of reward delivery (or expected reward delivery on error trials) was required to include a trial's SWRs (n=5 rats, error bars are s.e.m.).

(B) Changes in rewarded vs. error dSWR rate over task exposure, as a function of task epochs for each animal. Filled circles indicate mean dSWR rate across rewarded trials within the epoch (± s.e.m.), open squares indicate mean dSWR rate across error trials. Each point is color coded by the rewarded sequence of that epoch (Sequence A: orange; Sequence B: green). Black line indicates an exponential fit ± 95% confidence interval on error dSWR rate, grey line indicates exponential fit on rewarded dSWR rate.

(C) Changes in rewarded vs. error vSWR rate over task exposure for each animal shown in (**B**). Note that some error bars extend above the y-axis limit.

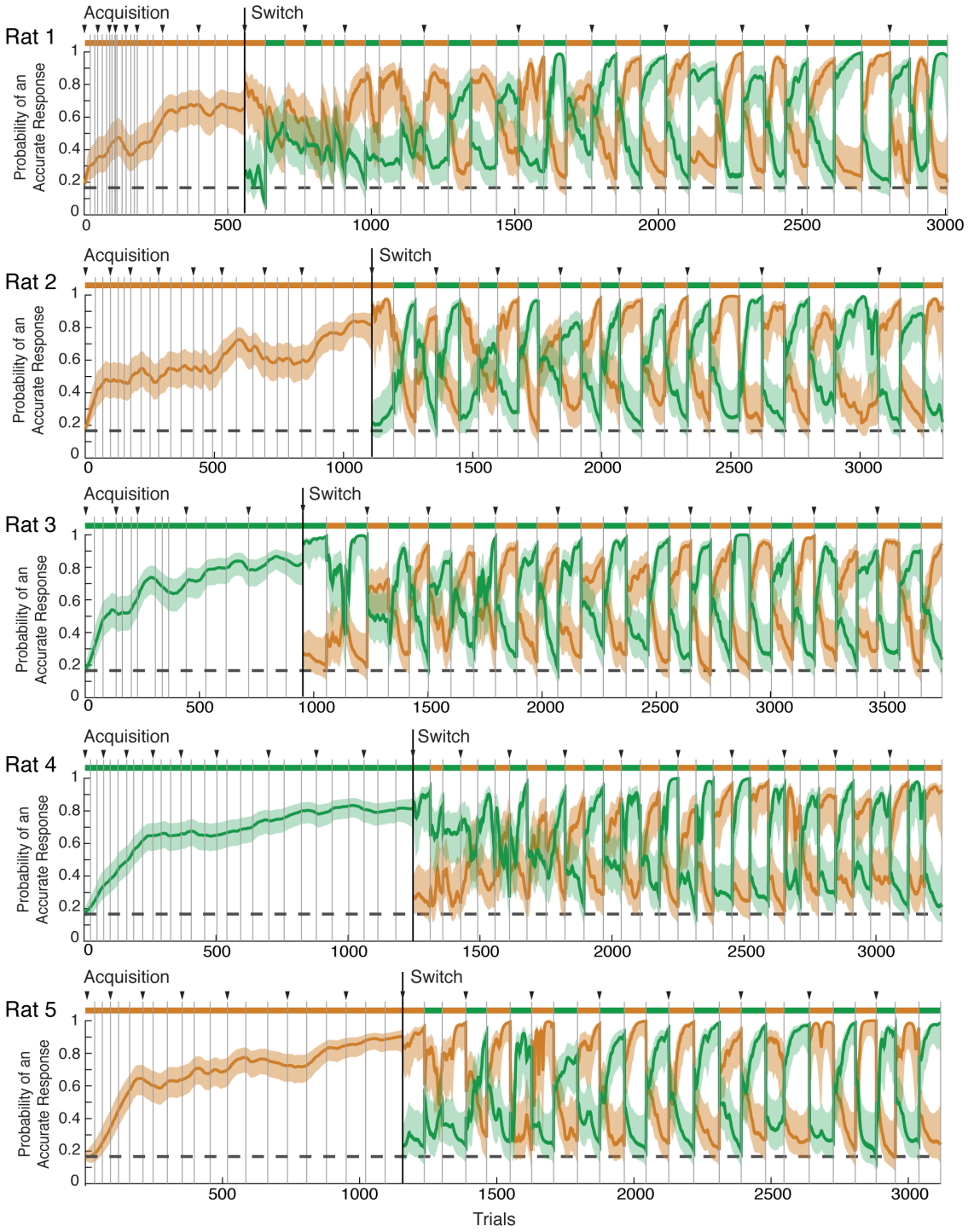

Figure S4. Multiple-W behavior, related to Figure 2.

Behavior from each rat expressed as the probability that the rat is making an accurate choice on each trial according to Sequence A (orange) or B (green) (see STAR Methods). Solid line indicates the mode of the probability distribution, shaded region indicates the 90% confidence interval. Colored bars at the top of each plot indicate the rewarded sequence, grey vertical lines mark epoch boundaries, black triangles mark the start of days, and the horizontal dotted line indicates chance performance: 1/6 (0.167).

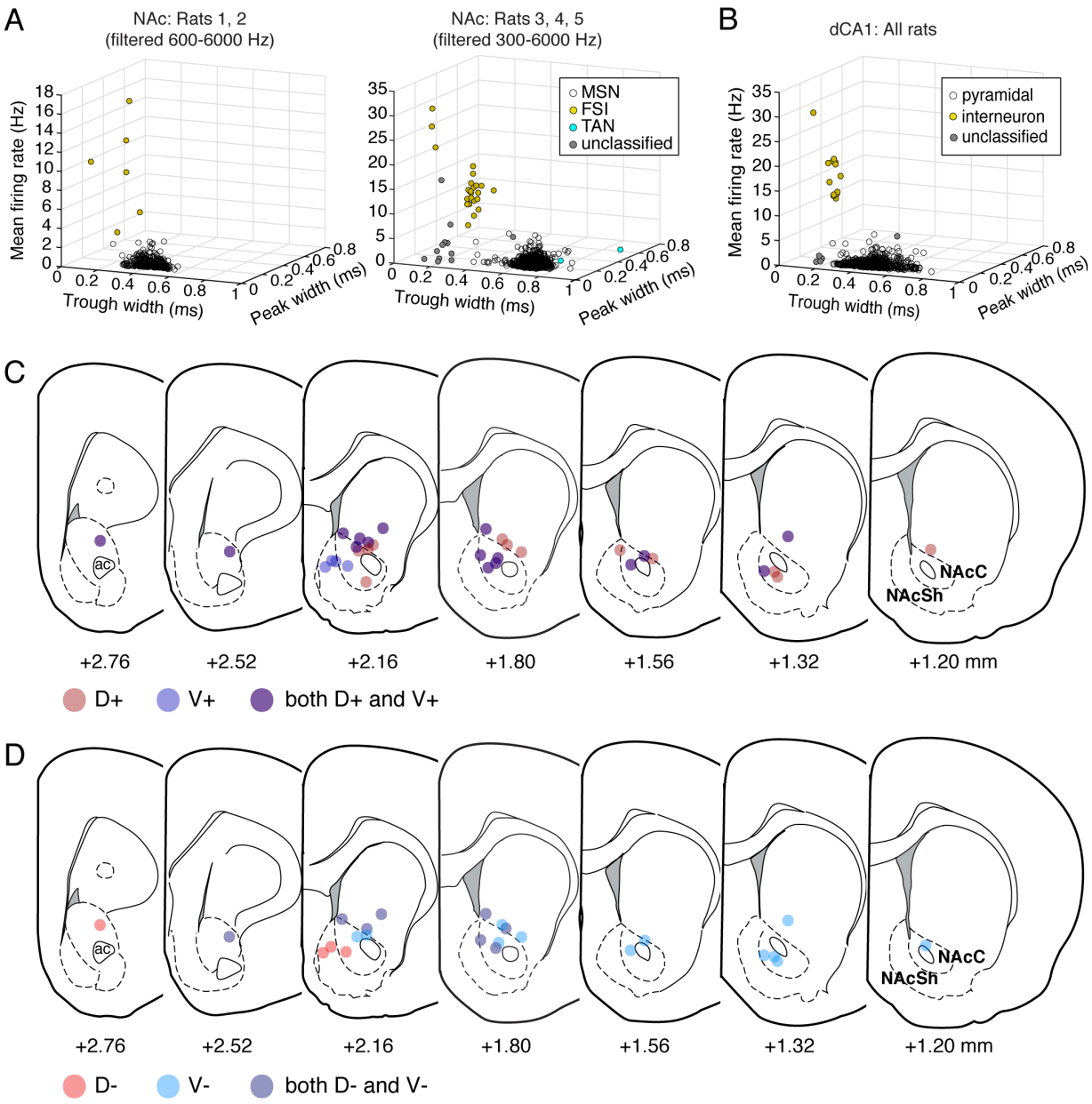

Figure S5. Cell type classification and mapping of awake SWR-modulated neurons in the NAc, related to Figure 3.

(A) Classification of putative NAc cell types by waveform properties and mean firing rate. Each point represents a single unit. Number of units (wake and sleep included): MSNs: 1799, FSIs: 30, TANs: 2, unclassified: 12. Data from Rats 1 and 2 (left) were classified separately from Rats 3-5 (right) due to narrower bandpass filtering at time of acquisition, as this changes waveform shape. Out of 1638 MSNs active during sleep, 718 were active only during sleep epochs and not during intervening run epochs, suggesting that only a fraction of the NAc population is active in our task.

(B) Classification of putative hippocampal cell types in dCA1. Number of units (wake and sleep included): pyramidal: 1218, interneuron: 13, unclassified: 18. dCA1 units contribute to Figure S6B,D and Figure 6D.

(C) Mapping of approximate tetrode locations where at least one D+ (dark red) or one V+ (dark blue) neuron (either MSN or FSI) was detected. All AP coordinates are in mm relative to Bregma and correspond to plate labels from the atlas (see Figure S1). Overlapping colors indicate locations where both D+ and V+ were detected, typically not in the same neuron. Note that borders of core (NAcC) and shell (NAcSh) are approximate, but that D+ modulation is limited largely to the dorsolateral core and its dorsolateral boundary, whereas V+ modulation is seen in the medial shell and also extends into the core.

(D) Mapping of approximate tetrode locations where at least one D- neuron (light red) or one V- neuron (light blue) was detected, again typically not in the same neuron. Note coincidence of D- sites with V+ sites and V- sites with D+ sites.

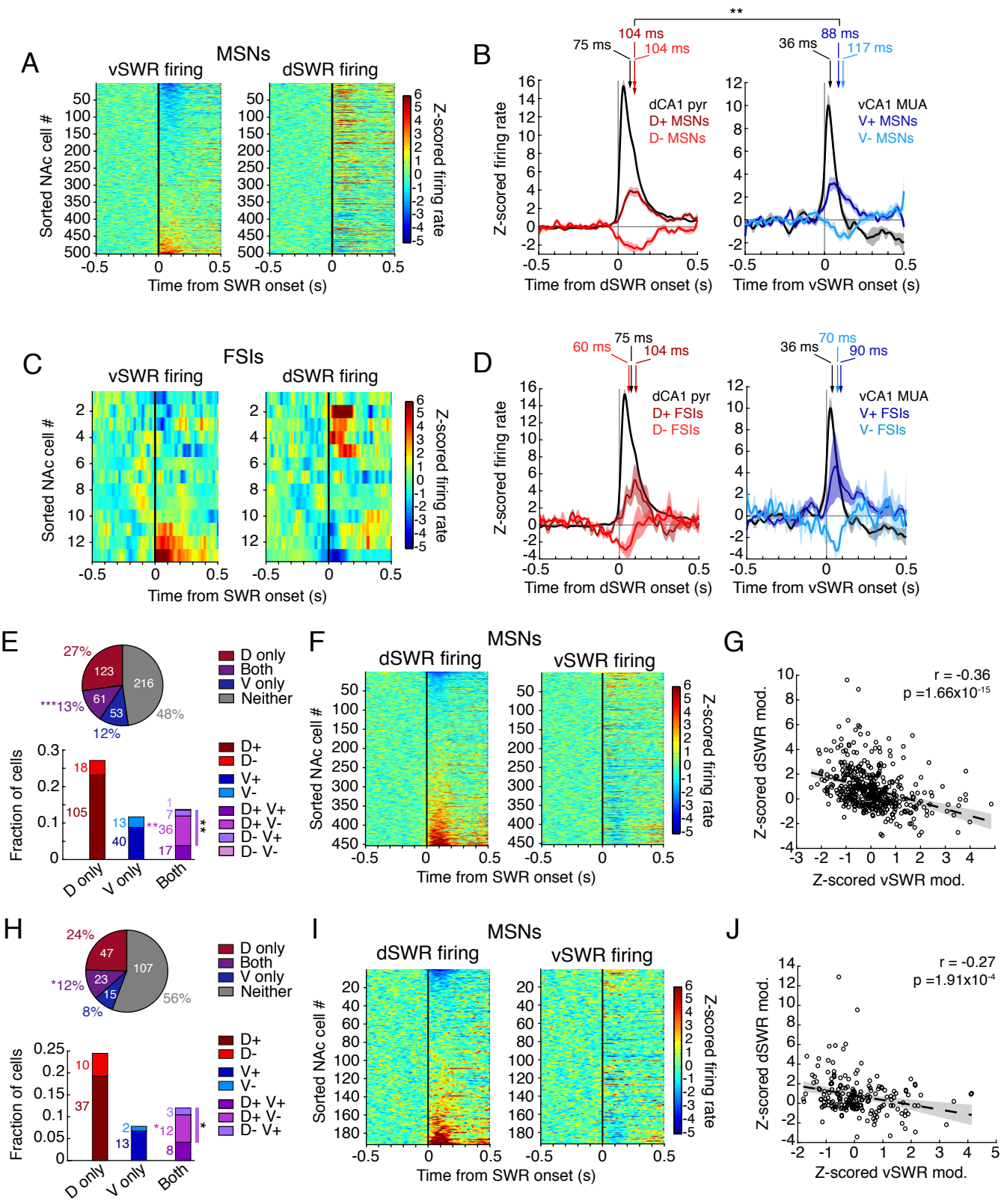
A
MSNs
vSWR firing
dSWR firing
Sorted NAc cell #
Z-scored firing rate
Time from SWR onset (s)
B
**
75 ms
104 ms
104 ms
36 ms
88 ms
117 ms
dCA1 pyr
D+ MSNs
D- MSNs
vCA1 MUA
V+ MSNs
V- MSNs
Z-scored firing rate
Time from dSWR onset (s)
Time from vSWR onset (s)
C
FSIs
vSWR firing
dSWR firing
Sorted NAc cell #
Z-scored firing rate
Time from SWR onset (s)
D
60 ms
75 ms
104 ms
36 ms
70 ms
90 ms
dCA1 pyr
D+ FSIs
D- FSIs
vCA1 MUA
V+ FSIs
V- FSIs
Z-scored firing rate
Time from dSWR onset (s)
Time from vSWR onset (s)
E
27%
123
216
***13%
61
53
48%
12%
D only
Both
V only
Neither
Fraction of cells
18
105
13
40
1
7
**36
17
**
D+
D-
V+
V-
D+ V+
D+ V-
D- V+
D- V-
D only
V only
Both
F
MSNs
dSWR firing
vSWR firing
Sorted NAc cell #
Z-scored firing rate
Time from SWR onset (s)
G
r = -0.36
p =1.66x10-15
Z-scored dSWR mod.
Z-scored vSWR mod.
H
24%
47
107
*12%
23
15
56%
8%
D only
Both
V only
Neither
Fraction of cells
10
37
2
13
3
*12
8
*
D+
D-
V+
V-
D+ V+
D+ V-
D- V+
D only
V only
Both
I
MSNs
dSWR firing
vSWR firing
Sorted NAc cell #
Z-scored firing rate
Time from SWR onset (s)
J
r = -0.27
p =1.91x10-4
Z-scored dSWR mod.
Z-scored vSWR mod.

Figure S6. NAc modulation during awake SWRs, related to Figure 3.

(A) Opposing modulation is not a result of cell ordering. Left: vSWR-aligned z-scored PETHs for each MSN ordered by its modulation amplitude (mean z-scored firing rate in the 200 ms following SWR onset). Right: dSWR-aligned z-scored PETHs for the same ordered MSNs shown on the left. Same MSNs as shown in Figure 3C.

(B) Timing of significantly modulated MSN ensemble activity, overlaid on dCA1 pyramidal cell firing (n=332 cells) during dSWRs (left) and vCA1 multiunit activity (n=4 rats) during vSWRs (right). Each curve represents the mean ± s.e.m. z-scored firing rate of the hippocampal (black), D+ (n=49 cells, dark red), V+ (n=16 cells, dark blue), D- (n=13 cells, light red), or V- (n=14 cells, light blue) populations. MSN subpopulations here are restricted to cells that passed the potential duplicate cell control. Arrows indicate the center of mass in the 0-200 ms post-SWR interval of each subpopulation's activity. The D+ center of mass occurs significantly later than the V+ center of mass (**$p<0.01$, permutation test). Timing difference of centers of mass of the D- and V- populations was not significantly different at the $p<0.05$ level. Also note that the centers of mass of the activated NAc ensembles lag the local activation of dH and vH neurons.

(C) Similar to **(A)** but for FSIs shown in Figure 3G.

(D) Timing of significantly modulated FSI ensemble activity during dSWRs (left), and vSWRs (right), overlaid on the same hippocampal activity as shown in **(B)**. Arrows indicate the center of mass in the 0-200 ms post-SWR interval of each population's activity; no significant differences in timing (permutation tests).

(E-G), Opposing MSN modulation cannot be accounted for by occasional co-occurrence of dSWRs and vSWRs (control for Figure 3B-D). Fraction modulated during Both: ***$p=9.13\text{x}10^{-4}$, fraction opposing: **$p=0.0046$, fraction D+V-: **$p=0.0089$ (z-tests for proportions).

(H-J), Opposing MSN modulation cannot be accounted for by inclusion of potential duplicate cells recorded across days (control for Figure 3B-D). Fraction modulated during Both: *$p=0.016$, fraction opposing: *$p=0.038$, fraction D+V-: *$p=0.046$ (z-tests for proportions).

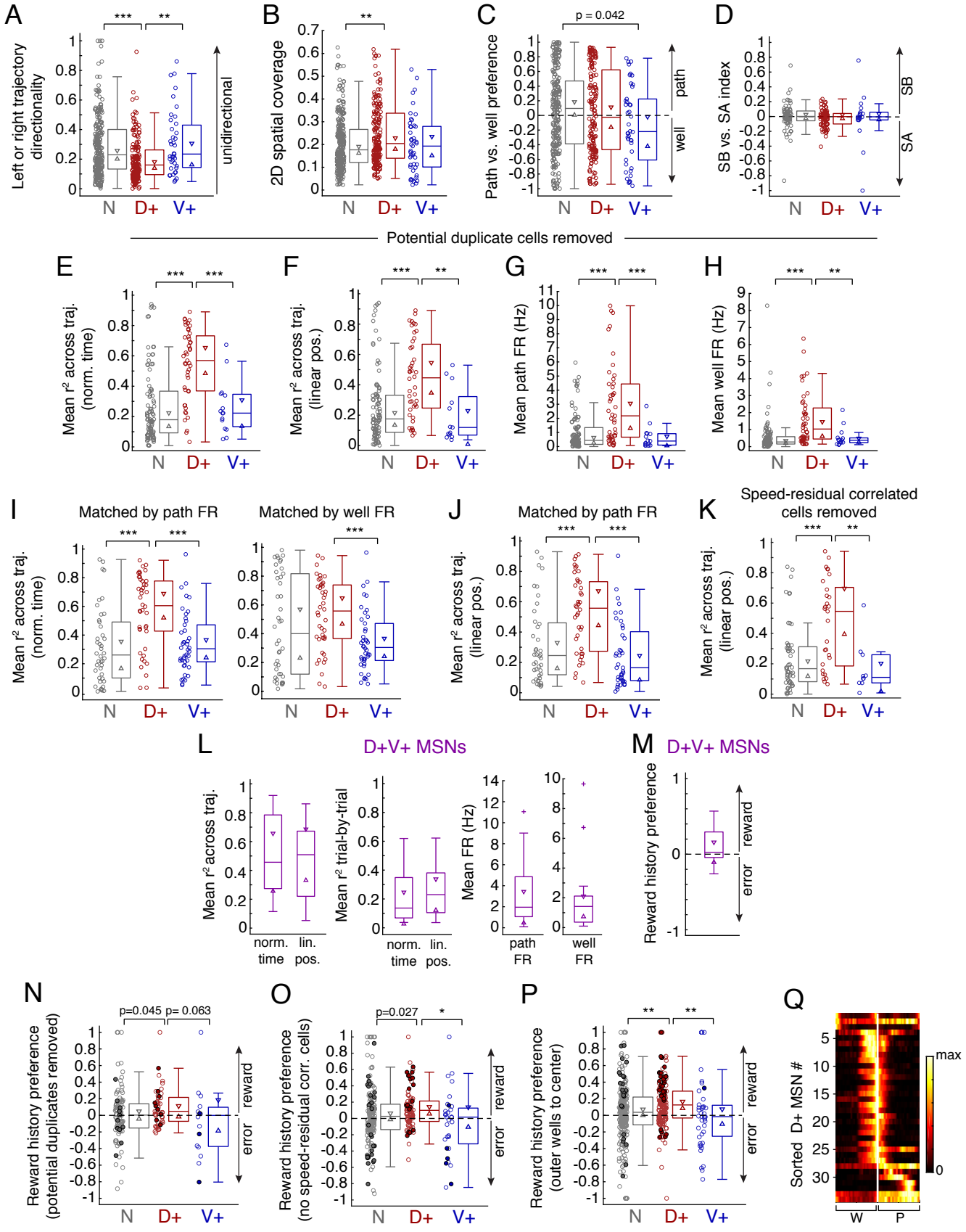
A
B
C
D
Left or right trajectory directionality
unidirectional
2D spatial coverage
Path vs. well preference
path
well
SB vs. SA index
SB
SA
N
D+
V+
***
**
p = 0.042
Potential duplicate cells removed
E
F
G
H
Mean r² across traj. (norm. time)
Mean r² across traj. (linear pos.)
Mean path FR (Hz)
Mean well FR (Hz)
I
J
K
Matched by path FR
Matched by well FR
Speed-residual correlated cells removed
L
M
D+V+ MSNs
Mean r² across traj.
Mean r² trial-by-trial
Mean FR (Hz)
norm. time
lin. pos.
path FR
well FR
Reward history preference
reward
error
N
O
P
Q
p=0.045
p= 0.063
p=0.027
*
Reward history preference (potential duplicates removed)
Reward history preference (no speed-residual corr. cells)
Reward history preference (outer wells to center)
Sorted D+ MSN #
max
0
W
P

Figure S7. Population task-related firing patterns of D+ and V+ MSNs, related to Figures 4 and 5.

(A) Directionality for either leftward- or rightward-moving trajectories, where 0 indicates bidirectionality and values closer to 1 indicate stronger unidirectionality. N (n=217 cells) vs. D+ (n=152 cells): ***p=9.56x10^{-6}; D+ vs. V+ (n=39 cells); **p=0.0013. All tests between populations in **A-K**, **N-P** are Wilcoxon rank-sum tests with Bonferroni correction for multiple comparisons, setting significance level at p<0.017.

(B) Two-dimensional spatial coverage of the environment, expressed as a fraction of occupied area on which cells fired >10% of their peak rate. N (n=246 cells) vs. D+ (n=161 cells): **p=0.008; D+ vs. V+ (n=45 cells): p=0.067.

(C) Preference for the path (>0) vs. well (<0) components of all trajectories. While individual cells exhibit strong preferences, the populations do not (N n=226 cells, D+ n=154 cells, V+ n=42 cells).

(D) Preference for Sequence B (>0) vs. Sequence A (<0) during correct and rewarded performance of that sequence. None of the populations exhibit preferences (N n=65 cells active during at least one epoch per rewarded sequence, D+ n=76 cells, V+ n=18 cells).

(E-H) Controls for Figure 4F,G,J,K with potential duplicate cells removed (see STAR Methods). In E, G, H: N n=93 cells, D+ n=45 cells, V+ n=15 cells; in F: N n=89 cells, D+ n=44 cells, V+ n=13 cells. **p<0.01, ***p<0.001.

(I) D+ MSN firing similarity across trajectories in normalized trial time is maintained when populations are matched for mean firing rate on the path (left: N vs. D+: ***p=1.18x10^{-4}; D+ vs. V+: ***p=1.22x10^{-4}) or well (right: N vs. D+: p=0.34; D+ vs. V+: ***p=4.17x10^{-4}; n=42 cells in each subpopulation).

(J) D+ MSN firing similarity across trajectories in linearized position is maintained when populations are matched for mean firing rate on the path (N vs. D+: ***p=5.23x10^{-4}; D+ vs. V+: ***p=4.54x10^{-6}; n=40 cells in each subpopulation).

(K) D+ MSN firing similarity across trajectories in linearized position is maintained when excluding cells with significant correlations between firing rate residuals and running speed residuals, where residuals are calculated between each trial and the mean of all trials. N (n=52 cells) vs. D+ (n=29 cells): ***p=7.96x10^{-4}; D+ vs. V+ (n=10 cells): **p=0.0036.

(L) D+V+ MSNs resemble D+ MSNs in task firing pattern properties (n=16 cells, related to Figure 4F,G,J,K). Crosses indicate outliers.

(M) Reward history preference of all D+V+ MSNs is not significantly greater than zero (n=16 cells, p=0.10, one-tailed signed-rank test).

(N) Control for Figure 5B with potential duplicate cells removed (N n=100 cells, D+ n=49 cells, V+ n=16 cells). D+ population is still significantly shifted greater than zero (p=0.0041, one-tailed signed-rank test).

(O) Control for Figure 5B removing cells with significant (either positive or negative) correlations between firing rate residuals and speed residuals. This aims to control for the possibility that consistent fluctuations in running speed between reward and error trials could account for reward history preference. The D+ population is significantly positively shifted, indicating reward

preference ($p=4.48x10^{-5}$, one-tailed signed-rank test). N (n=166 cells) vs. D+ (n=85 cells): p=0.027. D+ vs. V+ (32 cells): *p=0.01.

(P) Control for Figure 5B, examining only paths coming from the outer two wells to the center well of each rewarded sequence. This aims to control for upcoming choice and reward expectation, as returns to the center well are always rewarded. The D+ population is significantly shifted greater than zero ($p=3.75x10^{-9}$, one-tailed signed-rank test). N (n=222 cells) vs. D+ (n=158 cells): **p=0.0035; D+ vs. V+ (n=43 cells): **p=0.0076.

(Q) Ordered firing of D+ MSNs with significantly positive reward history preference on the path, as a function of normalized trial time. Mean well firing is included for illustration purposes only (W = well, P = path). The mean firing rate profile of each cell is calculated from all trials following reward across trajectories and normalized to the cell's maximum firing rate.

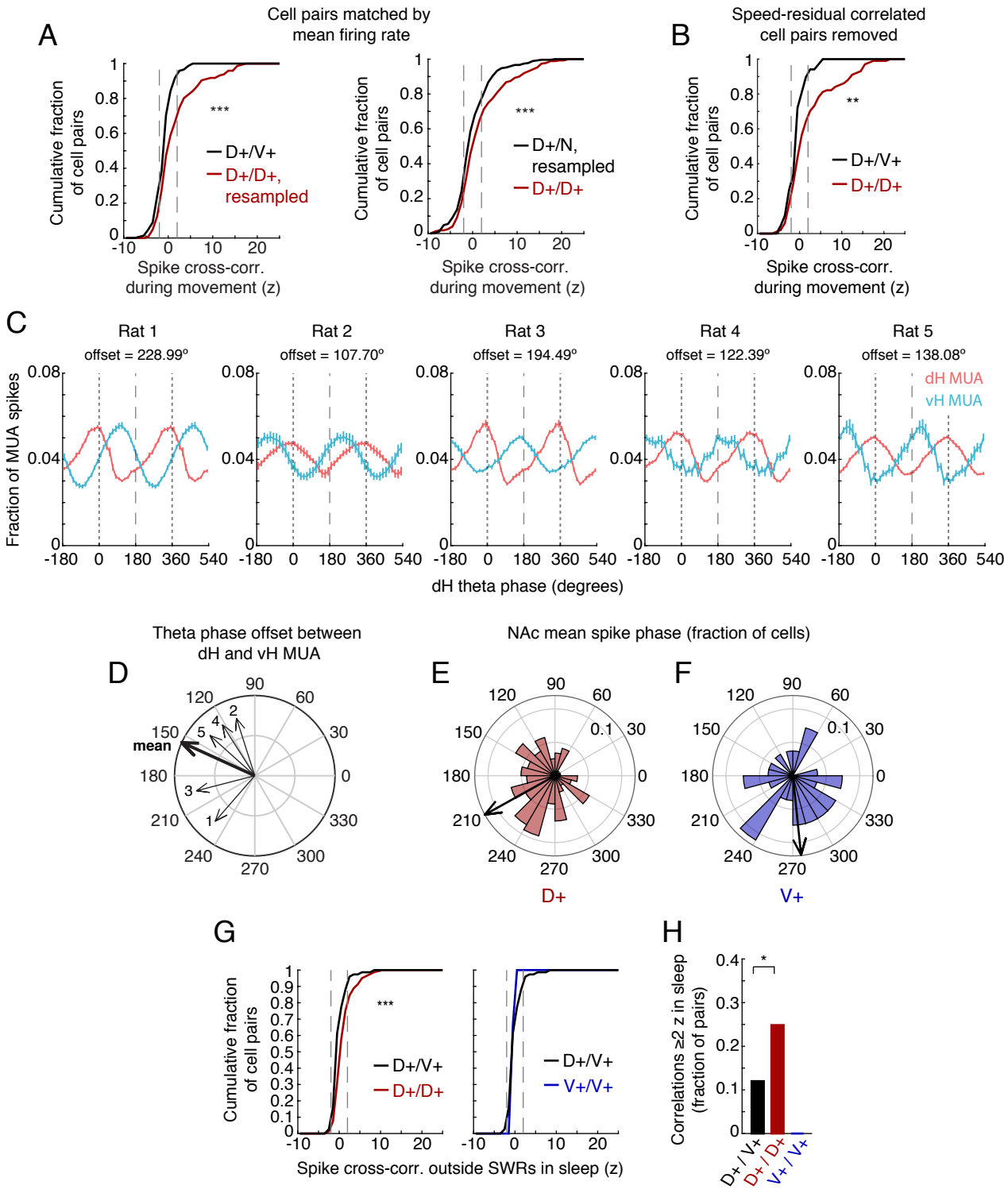
A
Cell pairs matched by mean firing rate
Cumulative fraction of cell pairs
Spike cross-corr. during movement (z)
D+/V+
D+/D+, resampled
D+/N, resampled
D+/D+
***
B
Speed-residual correlated cell pairs removed
**
C
Rat 1
Rat 2
Rat 3
Rat 4
Rat 5
offset = 228.99°
offset = 107.70°
offset = 194.49°
offset = 122.39°
offset = 138.08°
dH MUA
vH MUA
Fraction of MUA spikes
dH theta phase (degrees)
D
Theta phase offset between dH and vH MUA
mean
E
NAc mean spike phase (fraction of cells)
D+
F
V+
G
D+/V+
D+/D+
V+/V+
Spike cross-corr. outside SWRs in sleep (z)
H
Correlations ≥2 z in sleep (fraction of pairs)
D+ / V+
D+ / D+
V+ / V+

Figure S8. Asynchronous dH-NAc and vH-NAc network activity, related to Figure 6.

(A) Strong spike correlations between pairs of D+/D+ MSNs during movement cannot be explained by higher firing rates of D+ MSNs (control for Figure 6A). Left: pairs of D+/V+ MSNs versus pairs of D+/D+ MSNs that have been resampled to match the mean firing rates of D+/V+_ pairs (***$p=1.94x10^{-6}$, Wilcoxon rank-sum test; n=146 pairs in both populations). Right: pairs of D+/D+ MSNs vs. pairs of D+/N MSNs that have resampled to match the high mean firing rates of D+/D+ pairs (***$p=5.90x10^{-4}$, Wilcoxon rank-sum test; n=272 pairs in both populations).

(**B**) Strong spike correlations between pairs of D+/D+ MSNs cannot be explained the correlation of D+ activity with movement speed (control for Figure 6A). Pairs of cells were removed in which both cells had significant correlations between their firing rate residuals and running speed residuals in linear position. Remaining D+/D+ pairs (n=101 pairs) still show significantly higher spike cross-correlations at zero-lag compared to D+/V+ pairs (n=68 pairs); **p=0.0011, Wilcoxon rank-sum test.

(**C**) Mean dH (pink) and vH (blue) MUA aligned to dH theta for each animal (± s.e.m. across days, n=15-19 days per animal). Phase offset between MUA peaks, relative to vH MUA, is shown above each plot. Mean offset across days produces the arrows shown in (D). Two theta cycles are shown for clarity.

(D) Theta phase offset of dH and vH peak multiunit activity aligned to the dH theta rhythm, relative to vH MUA. Shorter arrows indicate the phase offset of individual animals, long arrow indicates the mean phase offset across animals (155.52 degrees, n=5; arrow length in arbitrary units). Angles are in degrees. Animal ID number is listed next to each arrow.

(**E**) Histogram of mean theta spike phase per D+ MSN (as compared to peak spike phase shown in Figure 6E-H). Length of bars indicates fraction of cells; note scale on grid. Arrow direction indicates mean phase preference of all D+ MSNs (209.05 degrees; arrow length in arbitrary units). n=118 D+ cells with significant theta phase modulation.

(**F**) Histogram of mean theta spike phase per V+ MSN. Length of bars indicates fraction of cells; note scale on grid. Arrow direction indicates mean phase preference of all V+ MSNs (275.92 degrees; arrow length in arbitrary units). n=27 V+ cells with significant theta phase modulation. Difference between mean phase preference of D+ and V+ cells = 66.88 degrees (p=0.0446, permutation test).

(G) Cumulative distributions of spike cross-correlations during sleep outside SWRs (mean at 0 ±10 ms, z-scored), between pairs of MSNs active in both wake and sleep, defined by D+ and V+ categories in wake. Left: pairs of D+ MSNs (D+/D+, n=161 pairs) vs. pairs of D+ and V+ MSNs (D+/V+, n=75 pairs). Right: pairs of V+ MSNs (V+/V+, n=3 pairs) vs. D+/V+ pairs. The D+/D+ distribution is significantly shifted to the right of the D+/V+ distribution (***$p=5.73x10^{-5}$, Wilcoxon rank-sum test), similar to wake. D+/V+ distributions are repeated from left to right for clarity.

(H) Fraction of cell pairs exhibiting positive spike cross-correlations (≥2 z-scores) in sleep outside SWRs. D+/D+ vs. D+/V+: *p=0.024; D+/D+ vs. V+/V+: p=0.32 (z-tests for proportions).